Hindawi Publishing Corporation
EURASIP Journal on Wireless Communications and Networking
Volume 2010, Article ID 290306, 15 pages
doi:10.1155/2010/290306

Research Article

Interference Mitigation between Ultra-Wideband Sensor Network and Other Legal Systems

Bin Li, Zheng Zhou, Weixia Zou, Feng Zhao, Zhuo Li, and Dejian Li

Wireless Network Laboratory, Key Laboratory of Universal Wireless Communications, Beijing University of Posts and Telecommunications, Ministry of Education (MOE), Beijing 100876, China

Correspondence should be addressed to Bin Li, stonebupt@gmail.com

Received 1 December 2009; Revised 26 January 2010; Accepted 11 March 2010

Academic Editor: Qilian Liang

Ultra-wideband impulse radio (UWB-IR) sensor network has intensive military and commercial applications. However, the interference between UWB and other existed networks should be casually investigated. In this paper, we consider interference mitigation in UWB sensors in the context of cognitive radio (CR). Firstly, we suggest a general state transition model to characterize the working states evolution of legal networks, also referred to as primary users (PU). Spectrum sensing, used to identify the state of PU, is formulated as detection of a corresponding state sequence. Maximum posterior probability (MAP) criterion is adopted to perform spectrum sensing. By exploring potential gain of state transitions, detection probability for nearby networks is improved significantly. Subsequently, based on the radius basis function neural network (RBF), we present a novel spectrum sculptor to design UWB waveforms. Attributed to the excellent reconfiguration of RBF, our scheme can produce UWB waveforms tracing available spectrums. The designed waveforms can entirely utilize multiple unoccupied bands to maintain uninterrupted communications. Also, sufficient spectral attenuation can be generated in specific bands to mitigate mutual interference between UWB sensors and other networks. Besides, orthogonal waveforms can be easily derived, which either improves transmission performance or provides a flexible accessing strategy for UWB sensors.

1. Introduction

Although the traditional Doppler radars have been commonly applied in perimeter monitoring systems, they will fail to detect the target and create coverage shadows when the protected area has obstacles or in a foliage. Additionally, a large object moving outside of the range of interest can create false alarms because of the limited range resolution of narrow-band radars, which cannot distinguish a nearby small target from another larger longer-range one. With a capability of excellent range resolution and penetration, on the other hand, UWB sensor radars have attached extensive investigations in recent years [1].

The emitted UWB signal occupies a tremendous bandwidth typically of several Gigahertz (GHz). Its fractional bandwidth is also very large, usually greater than 0.2, resulting in a sensor with exceptional resolution that also has the ability to penetrate many common materials. More importantly, such UWB sensors would be independent of Doppler shifts but would detect intrusion by measuring changes in the impulse response of environments. In [2, 3], UWB through-wall motion sensing radars and UWB ground penetrating radars (GPRs) are introduced to meet the requirements of special war field and the probe and rescue after a natural disaster. Recently, Liang et al. initiated the target detection in foliage using UWB radars and proposed that the log-logistic model was much suitable to represent UWB propagation channel in the foliage [4, 5]. Then, the sense-through-foliage target detection using UWB sensors is investigated in [6–8]. These researches significantly benefit the sense-through-wall and other subsurface sensing problems [9], which has become asymmetric threats in current and future military operational environments. Although the rapid progress in UWB research is originally inspired by radar sensors to a great extent, UWB sensor networks have also been widely recommended for different applications. For example, UWB network is an ideal candidate for short-range high-data-rate transmission which has been fully

discussed in the IEEE standard of wireless personal area network (WPAN), owing to its extremely wide bandwidth [10]. The energy efficiency issue in UWB network is also addressed through medium access control (MAC) protocol design in [11].

As the demand of data acquisitions and transmissions in various applications continues to grows, such as environment pollution sensing, intelligent traffic guiding, and remote medical monitoring, the current spectrum has become overcrowded and it is hard to allocate fixed frequency band to these new services. Accordingly, the trend of many networks for different purposes operating in nearby geographical regions seems inevitable. So, the interference mitigation and coexistence issues between UWB sensors and other networks should be carefully addressed. The UWB emission power regulation campaign error, launched by U.S. Federal Communications Commission, has been preceded for some years intending for interference mitigation [12]. However, this simple power control strategy does not seem sufficient for antagonistic cooperation between these networks [13].

In the emerging optimistic spectrum access infrastructure [14], by sensing and adapting to spectral environment, a cognitive UWB sensor is able to fill in spectrum holes and serves its users without causing harmful interference to other legal networks, which are also referred to as primary users (PUs) or authorized users. Correspondingly, signal detection here mainly aims to identify whether those perspective networks over UWB band are active, which is quite different from *target detection* discussed in most radar sensors-related literatures. From aspect of signal processing, the following two functional techniques should be thoroughly studied, in order to build a highly adaptive cognitive UWB sensor network that learns from the environment and best serves its users.

(1) *Spectrum Sensing*. A key element of UWB sensor network, in a cognitive paradigm, is the ability to measure, sense, and be aware of parameters related to the radio channel characteristics and availability of the spectrum. There have been some sensing algorithms including the energy detector (ED) [15], the matched filtering [16], and the cyclostationary detection [17], which have different requirements and advantages. ED is robust and simple but is unfavorable in the presence of noise uncertainty and interference [18]. Cyclostationary detection can differentiate PU from interference and noise; nevertheless, exhaustive search for unknown cyclic frequency makes it extremely computational and hence impractical. In matched detector, specific pilots are employed to achieve optimum detection SNR; however, perfect timing usually can hardly be achieved, which may greatly worsen detection performance. Recently, wavelet-based sensing algorithm is proposed in [19]. In [20], a novel sensing method is developed based on the statistical covariance of the received signal, which seems also immune to noise uncertainty.

(2) *Radio Emissions Strategy*. After identifying idle spectrums, UWB sensors need to take real-time adjustment on their emitting parameters to best match current spectral environment. Firstly, the transmit pulse should avoid primary bands to effectively mitigate mutual interference between UWB sensors and other networks. Also, the emitted waveforms should entirely utilize the idle spectrum bands in order to ensure communication reliability of UWB sensors. In [21], a novel UWB pulse shaping method based on prolate spheroidal wave functions (PSWFs) is presented. In [22], Gaussian Hermit functions (HGFs) are introduced to soft-spectrum waveform design, but the spectral efficiency is still unfavorable. The UWB shaping filter based on the second-order cone programming (SOCP) is proposed in [23, 24]; however, it is relatively hard to generate sufficient spectral notches to avoid other legal networks. Recently, a new spectrum forming technique based on transform domain communication system (TDCS) is presented in [25], which can design wideband waveforms according to identified idle spectrums. However, windowing process is indispensable in order to shorten the time domain waveform with an infinitely long tail that may introduce serious inter symbol interference (ISI). As a result, spectrum efficiency of TDCS will be considerably reduced and the out-of-band leakage becomes remarkable.

In this paper, we address the issue of interference mitigation in UWB sensor networks. Unlike the simple assumption that the working states between two adjacent sensing periods are independent, we employ a finite state machine to characterize PU's state transition. On this basis, we further model spectrum sensing as demodulation of a coded sequence with memory. After comprehensively balancing the cost between missing idle spectrums and causing interference to PU, in different applications, false alarm probability and missed detection probability are combined as the overall cost. From the aspect of minimizing the detection probability of *state symbols*, we then employ the maximum a posteriori criterion (MAP) to perform spectrum sensing. Compared with traditional sensing methods, our scheme can effectively explore potential gain carried by PU's working states and hence significantly reinforce sensing performance. We also reveal the rough interrelation between sensing performance and the potential information carried by PU and provide a new attractive pattern for future spectrum sensing which can be built into other algorithms to further enhance their detection probability.

Subsequently, based on radial basis function (RBF) neural network, we present a novel UWB waveforms generator with a versatile spectrum forming capability, which can produce the emitting signal effectively and flexibly. This scheme requires no frequency hopping between multiple isolated bands; thus it can considerably shorten switch time and reduce hardware complexity. The spectral attenuation of emitted signals can even reach 95 dB in corresponding primary bands, which can ensure the highly reliable

communications of other legal networks. Also, our designed UWB waveforms can entirely utilize uncontaminated idle spectrum and the whole spectral efficiency is up to 95%. Therefore, seamless data transmission for UWB users can be basically guaranteed. Meanwhile, by carefully designing the phase response of emitted signals, orthogonal pulses can be obtained which can greatly reduce mutual interference of UWB sensors and enhance the transmission performance of UWB networks, even when there is synchronization derivation. With the efficient self-adjusting algorithm and well-designed reconfigurability, our proposed spectrum sculpting technique totally meets the real-time and highly dynamic demands in cognitive UWB networks.

The remainder of this paper is outlined as follows. In Section 2, we discuss the system model of monitoring the other nearby networks. The working state evolution characteristics of PU is further introduced and an optimal sensing algorithm is proposed, in the sense that minimizing the detection probability, accompanying the robustness analysis of this sensing algorithm. A spectrum sculpting RBF is then proposed to design cognitive UWB waveforms with arbitrary spectrum shaping. Section 3 is dedicated to evaluate the sensing performance through numerical simulations. The performance of the designed UWB waveforms is also presented in this part. Finally, we conclude the whole paper in Section 4.

2. Cognitive-Based Interference Mitigation

In order to effectively mitigate interference between UWB sensors and other legal networks, from the signal processing aspect, two jobs can be suggested in consideration of the underlay nature of UWB. Firstly, UWB sensors accurately identify available spectrums by monitoring the nearby perspective networks. Then, based on the discovered spectral environment, they adjust the RF emissions to advantageously perform their functions, without interfering other networks [26]. These two functions will be elaborated in Sections 2.1 and 2.2, respectively.

2.1. Spectrum Sensing in UWB Sensors. In cognitive UWB sensors, spectrum sensing is mainly adopted to obtain the current states of other networks. Most traditional sensing schemes assume that whether the authorized users exist maintains independent between two adjacent detection periods, and the probabilities of active state and idle state remain the same. This processing strategy can greatly simplify the sensing algorithms; however, it also results in a suboptimal sensing performance.

Practically, the behavior of PU is close associated to its corresponding wireless service, leading to specific probability features on its working states to some extent. This potential information can be properly explored to improve sensing accuracy. There have existed a few literatures that seek to employ partial probability characteristics to enhance sensing performance [27, 28], including the optimization of spectrum detection scheduling to improve multiple channels utilization. Nevertheless, to the best of our knowledge, extensive investigation on spectrum detection by totally utilizing the state transition information of PU has not been addressed in the literature. The interrelation between sensing gain and the prior information also remains not discussed.

Our main contributions in spectrum detections may lie in that, for the first time, we model the working states of PU as a binary sequence characterized by finite state machine. Then, by fully exploring the potential information carried by PU, we employ MAP to perform optimal spectrum sensing and greatly enhance the detection performance. This processing strategy provides a novel insight into spectrum sensing, and our original revealment of the rough interrelation between the achieved sensing gain and PU's state transition characteristics may substantially benefit future researches in cognitive networks.

2.1.1. General Sensing Strategy. As UWB sensors cannot cause much interference to the authorized networks when using spectrum, they should search unused spectrum before establishing their data links. When specific unoccupied authorized band has been detected, the UWB sensor will send its data during the following time slot. However, since PUs may reclaim their spectrum at any time, UWB users should periodically sense the spectrum to avoid interfering nearby networks. So, we adopt the *cycle spectrum sensing mode* in this paper. The fixed frame duration F is assumed in which the sensing duration is T and the remaining duration F-T is used for data transmission [27]. It is noteworthy that the transmission here means either the data communications or some other dedicated functions, such as *target detection* and *positioning operations*.

Generally, cooperative sensing can alleviate the problem that one single sensor cannot detect the spectrum correctly when there is serious shadow fading [29]. If UWB sensors are taken into consideration, however, single node spectrum sensing is still a reasonable choice. Firstly, in a distributed UWB sensor network with highly dynamic characteristics caused by movement or birth-and-death process of sensor nodes, effective collaboration in spectrum sensing seems hard to be realized. Moreover, the required overhead may create heavy load for UWB network. The cooperative sensing even becomes impractical when the control channels are not available [30]. Additionally, the whole sensing time may become intolerantly long in a cooperative fashion. So, in this paper, we mainly focus on the single node spectrum sensing.

2.1.2. Energy Detection. Given the uncomplicated implementation of ED, it always remains the first choice for spectrum sensing in UWB sensors. Thus, this paper establishes the general sensing model based on ED. Before proceeding, it is necessary to briefly illustrate ED algorithm, which is always formulated as the following two hypotheses:

$$y(t) = \begin{cases} w(t), & H_0, \\ s(t) + w(t), & H_1, \end{cases} \tag{1}$$

where $y(t)$ is the received signal in UWB sensors, $s(t)$ is the nearby network's signal with its variance denoted by σ_s^2,

and $w(t)$ is the additive white Guassian noise (AWGN). In (1), H_0 and H_1 denote the hypotheses corresponding to the absence and presence of the primary networks, respectively. In realization, a band-pass filter is usually adopted to extract spectral components of interest. Then, the test statistics is constructed as the observed energy summation within M consecutive segments:

$$Y = \begin{cases} \sum_{m=1}^{M} |W(m)|^2, & H_0, \\ \sum_{m=1}^{M} |S(m) + W(m)|^2, & H_1, \end{cases} \tag{2}$$

where $S(m)$ and $W(m)$ $(m = 1, 2, \ldots, N)$ represent the spectral components of the primary signal $s(t)$ and $w(t)$ on the interested subband, respectively. Without loss of generality, we assume that $W(m)$ is white complex Gaussian noise with zero mean and variance σ_w^2. Then, the test statistics Y follows a central chisquare distribution with $2M$ degrees of freedom under H_0, and a noncentral chisquare distribution with $2M$ degrees under H_1, that is,

$$P(Y) = \begin{cases} N(M\sigma_w^2, 2M\sigma_w^4), & H_0, \\ N(M\sigma_w^2 + M\sigma_s^2, 2M\sigma_w^4 + 4M\sigma_w^2 N\sigma_s^2), & H_1. \end{cases} \tag{3}$$

If a decision threshold τ is properly determined, the false alarm probability P_f can be defined as $P(Y > \tau \mid H_0)$, and the corresponding detection probability P_d is $P(Y > \tau \mid H_1)$. Correspondingly, we have

$$\begin{aligned} P_f &= P(H_1 \mid H_0) = Q\left(\frac{\tau - M\sigma_w^2}{\sqrt{2M}\sigma_w^2}\right), \\ P_d &= P(H_1 \mid H_1) = Q\left(\frac{\tau - M\sigma_w^2 - M\sigma_s^2}{\sigma_w^2\sqrt{2M\sigma_w^2 + 4M\sigma_s^2}}\right). \end{aligned} \tag{4}$$

Accordingly, the missed probability is given by $1 - P_d$ [15]. $Q(\cdot)$ is the generalized Marcum Q-function which is given by

$$Q(x) = \frac{1}{\sqrt{2\pi}} \int_x^{+\infty} e^{-\tau^2/2} d\tau. \tag{5}$$

In practice, the probabilities of false alarm and missing detection have different implications for UWB sensors. Generally, low probability of false alarm is necessary to maintain high spectral utilization in UWB systems, since a false alarm would prevent the unused spectral segments from being accessed by UWB users. One the other hand, the probability of missed detection measures the interference of UWB users to PU, which should be limited in the opportunistic spectrum access. The most popular strategy is to determine a threshold to satisfy a false alarm probability, which is based on Neyman-Pearson criterion [27]. This scheme maximizes the detection probability for a given false alarm probability, for example, $P_f < 0.1$, which is suitable in most sensor networks. However, in some other scenes such as UWB radar sensors, the collected data for different vital applications should be transmitted without delay, which puts significant importance on spectral utilization, and the Neyman-Pearson criterion is not applicable anymore. Therefore, considering spectrum sensing by combining spectral utilization to unused bands and interference to PU, from a much wider sense, we minimize the total error probability in this paper. So the expense of spectrum sensing is given by

$$\Omega = 1 - P_d + P_f = P_m + P_f. \tag{6}$$

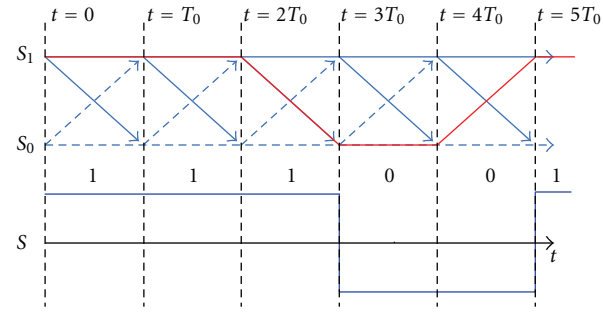

FIGURE 1: The trellis diagram for PU states transition. "1" represents the nearby network is active, while "0" denotes in idle.

2.1.3. State Transition of PU. For most wireless networks, the evolution process of their working states over time can be reasonably abstracted as a finite state machine. Specifically, as is shown in Figure 1, the state transition of PU can be described by a *trellis diagram* that is similar to NRZI code [31]. If PU is in active state S_1 at current moment, then in the next sensing slot, it will stay in S_1 with a probability of p_{11} and enter into sleep state S_0 with p_{10}. Alternatively, if it is current in sleep state S_0, then it will stay in S_0 in the next slot with a probability of p_{00} and change into S_1 with p_{01}. Obviously, we have:

$$p_{10} + p_{11} = 1, \qquad p_{01} + p_{00} = 1. \tag{7}$$

Usually, these transition probabilities vary with time. It is found that the state of authorized networks in each sensing duration corresponds with certain state symbol $s^{(t)}$ which constantly changes along the trellis diagram. Specifically, when the state transition occurs at $t = kT_0$, the following primary state keeps different from that in $[(k-1)T_0, kT_0]$. As the state transition further extended, $s^{(t)}$ can be viewed as a *BPSK coding sequence* with memory, which is also characterized by a *Markov chain*. Therefore, the main objective of spectrum detection lies in correctly demodulating this coded sequence $s^{(t)}$. Denoting the two states of PU as binary symbol "0" and "1", the optimum spectrum detection in (6) is equivalent to minimizing the symbol error probability (SER).

The MAP criterion can be properly employed in the successive symbol detection, which is optimum in the sense that it minimizes the detection probability of symbol errors [31]. Suppose that it is desired to detect the state symbol in the kth sensing duration, and let $[r_1 r_2, \ldots, r_k, \ldots, r_{k+D}]$ be the

observed test statistics, where D is the delay parameter which is always chosen to exceed the signal memory. If we denote the *inherent memory* of the equivalent sequence $s^{(t)}$ by L, then we have $D \geq L$. On the basis of the already received signal, we compute the posterior probability:

$$P\left(s^{(k)} = A_m \mid r_{k+D}, r_{k+D-1}, \ldots, r_1\right). \tag{8}$$

For possible state symbols $A_m \in \{0, 1\}$, we choose A_m with the largest probability. Then, we have

$$P\left(s^{(k)} = A_m \mid r_{k+D}, r_{k+D-1}, \ldots, r_1\right) = \frac{p\left(r_{k+D}, r_{k+D-1}, \ldots, r_1 \mid s^{(k)} = A_m\right) p\left(s^{(k)} = A_m\right)}{p(r_{k+D}, r_{k+D-1}, \ldots, r_1)}. \tag{9}$$

Since the denominator is common for two probabilities, the MAP criterion is equivalent to choose the value of $s^{(k)}$ that maximize the numerator of (9). Thus, the criterion for deciding on the kth state symbol is

$$\tilde{s}^{(k)} = \arg\left\{\max_{s^{(k)}} p\left(r_{k+D}, r_{k+D-1}, \ldots, r_1 \mid s^{(k)} = A_m\right) \times p\left(s^{(k)} = A_m\right)\right\}. \tag{10}$$

The solution for (10) recursively begins with the first symbol $s^{(1)}$; then the following state symbols $s^{(2)}, s^{(3)}, \ldots, s^{(k+D)}$ are sequentially obtained. The amplitude levels $\{A_m\}$ are only 2; so the computational complexity is basically acceptable. But, it is noteworthy that there exist fixed D delays in MAP algorithm. Consider that the idle spectrum may be reclaimed again during a short period, this presented detection algorithm with D accessing delays may miss most chances of using idle spectrum. Therefore, this original MAP-based sensing algorithm may not be appropriate to UWB sensors.

Furthermore, most recent research shows that the primary state of specific networks can be modeled as an *alternating renewal source*, in practice, which can be explored to simplify above MAP detection algorithm. As indicated by investigation in [32], the exponential distribution can be assumed for the probability density functions of the busy state and idle state periods as

$$f_{S_1}(n) = \frac{1}{\mu}\exp(-\mu n), \qquad f_{S_0}(n) = \frac{1}{\lambda}\exp(-\lambda n), \tag{11}$$

where μ and λ are the transition rates from busy to idle and from idle to busy, respectively. With the aid of *Komogorov Equation* [33], we obtain the probability of the idle state remaining unchanged during k successive detection periods:

$$p_{00}(k) = \frac{\mu}{\mu+\lambda} + \frac{\lambda}{\mu+\lambda}\exp(-k(\mu+\lambda)), \quad k = 1, 2, \ldots, \infty. \tag{12}$$

Similarly, the probability of the active state lasting for k detection periods is

$$p_{11}(k) = \frac{\lambda}{\mu+\lambda} + \frac{\mu}{\mu+\lambda}\exp(-k(\mu+\lambda)), \quad k = 1, 2, \ldots, \infty. \tag{13}$$

If we have identified the initial primary state in idle at the moment n_0, which means $p(s(n_0)) = 1$, then the probability that the primary state always stays in idle after k sensing transmission periods can be given by

$$p(s(n_0 + k) = 1) = p(s(n_0) = 1)\, p_{00}(k). \tag{14}$$

Accordingly, the probability of the primary state entering into busy in the kth detection period, after staying idle for $k-1$ periods, can be expressed as $1 - p_{00}(k)$.

It is noted from the above discussion that PU would stay in present state for certain sensing-transmission periods before jumping into another one. Thus, the key point of tracing a state path is to accurately determine the state transition moment. Furthermore, a careful observation on (14) shows that the state evolution following an exponential distribution has a limited memory, which means that the current state of authorized network is only related to the latest previous state rather than the upcoming ones. Based on these two points above, we may further simplify MAP algorithm in (10). If we have learned that the authorized user enters into state "1" at the moment $k - N + 1$ and stays for N periods, the optimal state estimation at the kth moment should meet

$$\tilde{s}^{(k)} = \arg\left\{\max_{s^{(k)}} p\left(s^{(k)} = A_m \mid Y_k, s^{(n)} = 1, n = k-1, \ldots, k-N+1\right)\right\}. \tag{15}$$

2.1.4. Spectrum Detection. In early stage, UWB sensors may take a long duration or employ some other sophisticated sensing algorithms (i.e., cyclostationary feature detection) to get the initial PU state correctly. Without loss of generality, supposing that the initial primary state is 0, then *a prior probability* of staying at this state for k sensing-transmission cycles is $p_{00}(k)$. In order to maximize a posteriori probability detection, (15) requires determining an optimum decision threshold τ_k^0 to meet

$$\frac{p_{00}(k)P\left(Y \mid s^{(k)} = 1\right)}{(1 - p_{00}(k))P(Y \mid s^{(k)} = 0)} = \frac{\alpha}{1-\alpha}. \tag{16}$$

Here, α is the weighting coefficient ranging in [0 1], which can be carefully used to adjust relative preference between missed probability and detection probability. In practice, $\alpha > 0.5$ means the cost of spectral efficiency decline because a missed detection is relatively larger than that of interfering the PU, which implies that the nearby networks possess a strong anti-interference ability. In this situation, we may aggressively improve the utilization efficiency of idle spectrums to facilitate data transmissions of urgent UWB applications. On the other hand, $\alpha < 0.5$ implies that we show much favor to the unperturbed communication link of PU compared to the spectrum efficiency. Hence, strict protection to the authorized networks is necessary.

After the optimum decision threshold has been obtained according to (16), the detection probability P_0 in the kth moment can be given by

$$P_0 = P\left(Y < \tau_k^0 \mid s^{(k)} = 0\right). \tag{17}$$

Similarly, the threshold for initial state 1, τ_k^1, can be also obtained. Then, the detection probability P_1 can be written as

$$P_1 = P\left(Y > \tau_k^1 \mid s^{(k)} = 1\right). \tag{18}$$

Since the state symbol may not appear equally, the overall probability of correct detection is

$$\begin{aligned} P_c = {} & \frac{\mu}{\mu+\lambda}\frac{\sum_k p_{00}(k)P\left(Y < \tau_k^0 \mid H_0\right)}{\sum_k p_{00}(k)} \\ & + \frac{\lambda}{\mu+\lambda}\frac{\sum_k p_{11}(k)P\left(Y > \tau_k^1 \mid H_1\right)}{\sum_k p_{11}(k)}. \end{aligned} \tag{19}$$

It is obvious that maximizing P_c gives the minimum sensing expense Ω. Actually, from the information theory aspect, spectrum sensing is equal to detecting a binary-coded sequence that obeys an unsteady state transition, given the reward of detection probability and missed probability. Like in most traditional spectrum sensing algorithms, if two sequential states of authorized users are simply assumed to be independent, the detection probability would be rather limited. However, our MAP-based optimum spectrum sensing is supposed to be much superior to ED, in consideration of entire exploration of the implicit state evolution and corresponding potential *coding gain*. Compared to matched algorithm and cyclostationary detection, our method only requires a statistic traffic model rather than the specific signal parameters of different networks, which can be conveniently obtained by experiential data or by learning.

2.1.5. Robustness Analysis. When the last state transitions of PU are exactly estimated, the simplified algorithm is equal to MAP algorithm, and it has optimal detection performance. However, from (16), spectrum detection errors in state transition moment will cause error extension in the upcoming periods. To avoid this unfavorable situation, following measures are suggested when PU has entered one state and lasted beyond its mean duration. (1) We may change the relative ratio between sensing period and transmission period. In an extreme case, the whole cycle is allocated for spectrum detection. (2) Other advanced sensing algorithms can be employed to assist estimating the exact state transition. (3) After n sensing-transmission periods, usually n being among 5–10, we may employ the *truncated sequential detection* and retake a long duration to detect the initial state and then repeat this process.

The bad effect on detection probability caused by state transition estimation errors will be discussed in this part, which is instructive if these suggested measures cannot be realized. In the situation with low detection probability, the state transition point can be correctly estimated by adjusting sensing duration. Compared to ED, however, detection gain in this case is quite limited but with a high complexity. So, we mainly analyze the performance decline caused by the state transition estimation errors under high detection probability. Assuming that the average detection probability is p, in the worst case, the detection error occurs successively, whose length is about $(1-p)\times(1/\lambda+1/\mu)$.

Firstly, we focus on state detection errors that occur near the actual state transition point, which has a serious influence on the upcoming detections. For convenience, suppose that the estimation errors take $(1-p)\times(1/\lambda+1/\mu)$ detection cycles in advance the actual transition moment, which is referred to as advanced transition detection error (ATDE). Given that the initial state is 0, accordingly, affected by this error initial state, subsequent optimum thresholds are determined by

$$\frac{p_{00}(k+(1-p)(1/\lambda+1/\mu))P\left(Y \mid s^{(k)}=1\right)}{[1-p_{00}(k+(1-p)(1/\lambda+1/\mu))]P(Y \mid s^{(k)}=0)} = \frac{\alpha}{1-\alpha}. \tag{20}$$

The thresholds in following decision are denoted by $\tau_{k+(1-p)(1/\lambda+1/\mu)}$, and the corresponding detection probability is

$$\begin{aligned} P_{\mathrm{APDE}} = {} & \frac{\mu}{\mu+\lambda}\frac{\sum_k p_{00}(k)P\left(Y < \tau^0_{k+(1-p)(1/\lambda+1/\mu)} \mid H_0\right)}{\sum_k p_{00}(k)} \\ & + \frac{\lambda}{\mu+\lambda}\frac{\sum_k p_{11}(k)P\left(Y > \tau^1_{k+(1-p)(1/\lambda+1/\mu)} \mid H_1\right)}{\sum_k p_{11}(k)}. \end{aligned} \tag{21}$$

Secondly, we investigate the nonideal case that the worst estimation errors occur in the middle of state transition (MPDE); namely, the estimated transition moment is much earlier than the actual state transition. In order to avoid this false state transition, ED is preferred to MAP detection in (15) after the false state estimation has occurred. Then, a counter is adopted for the sustaining periods of this false state. If the sustaining periods are smaller than $(1-p)\times(1/\lambda+1/\mu)$, we may conclude that the state transition does not actually occur and the upcoming detection still follows the correct state before. If it is larger than $(1-p)\times(1/\lambda+1/\mu)$, then we judge that the state transition indeed happens, and the current sustaining period of this new transited state is set as $(1-p)\times(1/\lambda+1/\mu)$. It can be easily found that the detection error is not diffusive in this way; thus the upcoming sensing performance is basically not affected. When $(1-p)\times(1/\lambda+1/\mu)$ is far less than $\min(1/\lambda, 1/\mu)$, the detection probability low-bound can be approximated by

$$\begin{aligned} P_{\mathrm{MPDE}} = {} & \frac{\mu}{\mu+\lambda}\left[(1-p)\left(1-P_f^{\mathrm{ED}}\right)+p\left(1-P_f\right)\right] \\ & + \frac{\lambda}{\mu+\lambda}\left[(1-p)\left(1-P_m^{\mathrm{ED}}\right)+p(1-P_m)\right], \end{aligned} \tag{22}$$

where P_f^{ED} and P_m^{ED} represent the probabilities of false alarm and missed detection of ED algorithm, respectively.

The analysis above provides the detection performance in the case that the false state estimations cause error diffusion during following detections. However, it is also noteworthy that the successive estimation errors of $(1 - p) \times (1/\lambda + 1/\mu)$ are almost impossible to happen; so our analysis only provides a loose *low bound* for sensing performance with state estimation errors under high detection probability.

2.2. Spectrum Sculpting in UWB Sensors. Detecting the presence of other nearby networks in a given primary band is just the first step in operation of a cognitive UWB sensor. In order to best adapt to current spectral environment and minimize mutual interference, UWB sensors should dynamically adjust the RF emissions after probing the current spectrum. Usually, this process covers the physical layer design as well as the upper layer joint optimization. Cross layer optimization is recommended for selecting transmission parameters according to the upper layer quality of service (QoS). Unfortunately, this process is basically computational and also has intolerable delay in practice. In contrast, the UWB waveform designing rarely considers QoS information from the upper layer, but this flexible strategy allows the simple implementation and fast accessing to idle spectrums and hence is much more suitable for distributed UWB sensors.

2.2.1. RF Requirements in CR. Based on an overall consideration of various factors, UWB waveforms design should meet the following requirements.

(1) *Avoid the licensed frequency band flexibly and effectively*. It is possible to avoid authorized frequencies based on frequency hopping technique [34]; but in this mechanism, UWB sensors can only use one single free band, resulting in rather low spectrum utilization. In addition, oscillator operating at multiple frequencies is required, which also complicates the hardware implementation. Moreover, the switching time for typical PLL can even reach 1 ms, which may prevent UWB sensors from the timely utilization of idle spectrum. On the other hand, spectrum avoidance-based schemes have a limited spectral attenuation, which can hardly eliminate the accumulated interference from multiple UWB sensors to other networks [21, 22].

(2) *Use the idle spectrum entirely*. Generally, more than one free spectrum hole exist, which always isolates a long spectral distance from each other. The traditional methods can use only one free band. Considering the high uncertainty of authorized band, data transmission of UWB nodes is easy to be interrupted by the reclaim of primary band. In order to ensure seamless communications, UWB sensors should utilize multiple idle bands simultaneously in case one PU reoccupies its primary band. TDCS can take advantage of multiple frequency bands. But, the designed waveform has an infinite long tail which inevitably causes ISI and hence undermines its transmission performance. Yet, truncation by windowing will in turn lead to an obvious degradation on spectral efficiency and remarkable out-band leakage [25].

(3) *Simplify the upper layer design*. Most of traditional spectrum access strategies are based on competitive mechanism or centralized scheduling. On one hand, it has to occupy remarkable bandwidth resource to pass the global control signaling. On the other hand, it also has to take a long time to coordinate transmission of each UWB node, which also inevitably misses most spectrum holes.

In this part, we suggest a novel UWB waveform based on the RBF neural network. The designed signal is highly reconfigurable which can entirely match target spectrum shape after an extremely short switching time. Also, efficient spectral attenuation can be produced to eliminate mutual interference between PU and UWB sensors. After the spectral holes have been identified based on our presented sensing algorithm, UWB sensors can immediately access in the following transmission slot by means of orthogonal waveforms, without waiting for a coordination control. Thus, the upper layer control can be considerably simplified, and the UWB sensors capacity can be enhanced at the same time.

2.2.2. System Architecture. With the excellent capability of the function approximation, RBF neural network can be properly applied to design UWB waveforms given any target spectrum shaping [35]. The main philosophy behind RBF is to adjust a set of basis functions and ultimately match any function in high dimension, at any precision. In fact, as pointed out in [36], the general spectrum forming can be viewed as two-dimensional multivariable interpolation problem, which means that given a set $\{f_i \in R_1 \mid i = 1, 2, \ldots, N\}$ containing N different frequency values and another set $\{t_i \in R_1 \mid i = 1, 2, \ldots, N\}$ containing N sampled target spectrum values, the objective is to find a mapping function $F : R_1 \to R_1$ to meet

$$F(f_i) = t_i, \quad i = 1, 2, \ldots, N, \tag{23}$$

where f_i represents the ith discrete frequency value, and t_i is the corresponding sampled spectrum. With the help of the continuity of mapping function, spectrum values other than f_i can be also obtained. If a set of basis functions $\varphi(\|f - f_i\|)$ are properly chosen, then the mapping function can be represented as a linear combination of the basis functions:

$$F(\mathbf{f}) = \sum_{i=1}^{N} w_i \varphi(\|f - f_i\|). \tag{24}$$

In UWB waveform designing, the selection of basis functions $\varphi(\|f - f_i\|)$ is rather different from the traditional sense. Since the basis functions mainly act as the interpolation functions, they are not required to keep orthogonal from each other. When selecting basis functions, it should ensure the localization property firstly, which means $\lim_{r \to 0} \varphi(r) \to 0$. Meanwhile, the basis functions should be central even

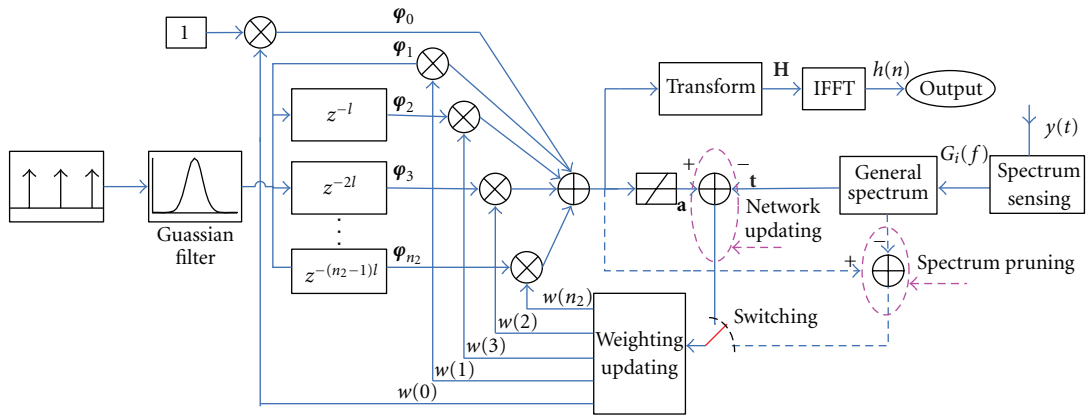

FIGURE 2: The structure of the UWB spectrum shaping network. Note that the result of spectrum sensing determines the current expected output.

symmetry, for example, $\varphi(-r) = \varphi(r)$. Besides, they should satisfy the requirement as indicated by Micchelli Theorem [37]. For the convenience of analysis, Gaussian function is served as the basis function in our following analysis; however, other candidate functions meeting above requirements include the raised cosine function and the exponential function [35]:

$$p_i(k) = \frac{1}{\sqrt{2\pi}\delta_i} \exp\left(-\frac{f_s^2}{2\delta_i^2}(k-\kappa_i)^2\right), \quad k = 0, 1, \ldots, N-1, \ i \neq 0, \tag{25}$$

where κ_i and δ_i are both adjustable parameters of the transmission functions T_i, which can be employed to modify their center and width, respectively; f_s is the sampling interval in frequency domain.

The implementation architecture of the generalized spectrum shaping network is shown in Figure 2. Based on the spectrum sensing result in Section 2.1, the target output **t** can be firstly determined with a purpose of fully utilizing unoccupied spectrums and also respecting the active primary bands. Then, the parameters of RBF network, including the network weight **w**, the position, and shape of basis functions, are modified adaptively until the error signal between the network output **a** and the expected output **t** reaches the minimum value. This adjusting process is shown by the solid line in Figure 2. Meanwhile, by introducing the spectrum pruning technique, further slight adjustments will be performed on partial network weigh **w** after convergence, so as to obtain satisfactory spectrum efficiency and also meet specific spectrum constraints. This process corresponding to this feedback process is depicted by the dotted line, which is controlled by a switching circuit.

Each part of signal is discussed in detail as follows.

(1) Transform Function $\mathbf{T}_i$. Transmission functions $\mathbf{T}_i$ are mainly used to produce the discrete input sequence $\varphi_i(n)$ $(n = 0, 1, \ldots, N-1;\ i = 0, 1, \ldots, n_2)$, which corresponds to the basis functions in (25). Supposing that $\boldsymbol{\varphi}_i$ denotes an $N \times 1$ dimensional vector composed of $\varphi_i(n)$, then the input matrix $\boldsymbol{\Phi}$ can be written as

$$\boldsymbol{\Phi} = \left[\boldsymbol{\varphi}_0\ \boldsymbol{\varphi}_1\ \boldsymbol{\varphi}_2\ \cdots\ \boldsymbol{\varphi}_{n_2-1}\ \boldsymbol{\varphi}_{n_2}\right]^T, \tag{26}$$

where $\boldsymbol{\varphi}_0$ represents the network offset. In the block diagram above, the transmission function $\mathbf{T}_i$ has to be implemented by the group of filters in practice, and the time bandwidth product BT of these Gaussian filters is determined by δ in (25). Note that the number of transform functions is always less than N in order to simplify implementations [37].

(2) Target Output **t**. The target output **t** corresponding to the optimal emission spectrum depends on the current spectral environment. If we assume that there are total I kinds of active legal systems, then the expected spectrum can be expressed as

$$\mathbf{t} = \prod_{i=1}^{I}(1 - G_i(f))\Big|_{f=kf_s} \quad k = 0, 1, \ldots, N-1, \tag{27}$$

where $G_i(f)$ represents the indication gating function corresponding to the ith kind of PU. If the legal network locating at $[f_{i1}, f_{i2}]$ has been detected using the sensing method in Section 2.1, then the associated gating function $G_i(f)$ is enabled:

$$G_i(f) = \begin{cases} 1 & f \in [f_{i1}\, f_{i2}] \text{ and } s_i(t) = 1, \\ 0 & f \notin [f_{i1}\, f_{i2}] \text{ or } s_i(t) = 0, \end{cases} \tag{28}$$

where $s_i(t)$ represents current working state of the ith PU.

(3) Parameters Updating. During the parameters adjustment process, by adaptively changing the network weights **w** and the transmission parameters κ_i and δ_i, the mean square error (MSE) between the actual output **a** and the target output **t** will be minimized. And finally, we obtain the UWB signal with optimal spectrum shaping. The MSE can be defined as

$$E = \frac{1}{2}\|\mathbf{a} - \mathbf{t}\|_2^2 = \frac{1}{2}\sum_{k=0}^{N-1}\sum_{i=0}^{n_2}[w(i)\varphi_i(k) - t(k)]^2, \tag{29}$$

where the coefficient 1/2 is just for facilitating the elaboration. The parameters updating of this UWB waveform generator, including the network weights and transmission parameters, can be divided into two phases [37]. The network weights $\mathbf{w}$ are firstly adjusted using Windrow-Hoff rule. Then, the transmission parameters κ_i and δ_i can be modified by resorting to the gradient descent rule. Correspondingly, the partial derivatives of E on transmission para meters can be written as

$$\begin{aligned}\frac{\partial E}{\partial \kappa_i} &= \sum_{k=0}^{N-1}\sum_{i=0}^{n_2} w(i)\left[w(i)\varphi_{\mathbf{i}}(k) - t(k)\right]\frac{\partial \varphi_{\mathbf{i}}}{\partial \kappa_i},\\ \frac{\partial E}{\partial \delta_i} &= \sum_{k=0}^{N-1}\sum_{i=0}^{n_2} w(i)\left[w(i)\varphi_{\mathbf{i}}(k) - t(k)\right]\frac{\partial \varphi_{\mathbf{i}}}{\partial \delta_i}.\end{aligned} \tag{30}$$

(4) Implementation. In UWB sensors applications, the duration of the learning algorithm directly determines the accessing delay to idle spectrums. Therefore, we need to optimize the transmission parameters beforehand to further shorten the switching time, also simplifying the implementation of UWB nodes.

In fact, when n_2 is big enough, we may let each κ_i evenly distributed in frequency axis and employ one single Gaussian filter to generate the basis function $\boldsymbol{\varphi}$. Then, the other basis functions $\boldsymbol{\varphi}_i$ can be obtained by $l \times i$ samples cycle shifting operation on $\boldsymbol{\varphi}_1$, where l represents the shifting factor ($l > 1$). So we can further optimize the single parameter δ. A reasonable parameter δ should actually be neither too large to avoid serious ripples in the pass band nor too small in case that the designed waveform has an obvious out-band leakage which may interfere PU in adjacent band [35].

Based on the above simplification efforts, the structure of UWB pulse generator can be obtained as is shown in Figure 2. Firstly, an impulse sequences with a period of N is produced, which is then fed into a Gaussian shaping filter whose key parameter, the time-bandwidth product BT, is determined by the already optimized δ. Then the network basis function $\varphi(n)$ can be formed. The sampling frequency of $\varphi(n)$ is set to $2f_{\max}$, where $f_{\max}$ is the maximum frequency of UWB signals. After that, the network input sequences $\varphi_i(n)$ can be constructed after $i \times 8$ ($i = 0, 1, 2, \ldots, n_2$) samples delay has been performed on $\varphi(n)$. Notice that, here, sample delay is equivalent to cycle shift considering the periodic input impulse sequence. Finally, in the updating stage, the UWB waveform shaper makes adjustment to its weighting vector $\mathbf{w}$ according to target output $\mathbf{t}$ that relies on nearby spectrum environment.

When the RBF network is directly applied to UWB sensors, it is usually difficult to meet some given spectral constraints. For example, the designed UWB waveforms under specific spectral masks will have some serious mismatch near the abrupt spectral edges [35]. This would bring in serious negative effects in cognitive scenarios and reduce its applications significantly. Assuming that there is a spectral mismatch during the frequency band $[f_{\text{down}} f_{\text{up}}]$, then the corresponding network weight subset is denoted by $\mathbf{w}_{\text{sub}} = \{w_k : m \le k \le n\}$, where m and n can be obtained by

$$m = \left\lfloor \frac{f_{\text{down}}}{(l \times f_s)} \right\rfloor, \qquad n = \left\lceil \frac{f_{\text{up}}}{(l \times f_s)} \right\rceil. \tag{31}$$

The main objective of the spectrum pruning is to repair the remarkable local spectral mismatch. This process is also iterative, and the basic idea is to further modify the converged network weights falling into the mismatch range. When n_2 is large enough ($n_2 > 60$) and the maximum tolerance of the spectral mismatch is denoted by ξ, the spectrum pruning can be summarized into

$$w_i^{(k)} = \begin{cases} \eta w_i^{(k-1)}, & i \in [m,n] \text{ and } H^2(f) - M(f)\big|_{f=[f_{\text{down}} f_{\text{up}}]} \ge \xi \\ w_i^{(k-1)}, & i \in [m,n] \text{ and } H^2(f) - M(f)\big|_{f=[f_{\text{down}} f_{\text{up}}]} \le \xi \\ w_i^{(k-1)}, & i \notin [m,n], \end{cases} \tag{32}$$

where η is the pruning step. $H(f)$ represents the UWB emission spectrum obtained from this shaping network, and $M(f)$ is the regulatory spectral constraint. This iterative spectrum pruning process will be continued until all frequency bands have met the given spectral constraints.

2.2.3. Orthogonal Pulse Design. After both the network weights and the transmission parameters have converged to their optimal solutions, the frequency response of the designed signal can best approximate to the expected spectrum. So, we may immediately produce the UWB waveform by IDFT on $\mathbf{a}$:

$$\begin{aligned} h(n) &= \text{IDFT}\left(\left[\!\left[\exp(j2\pi\Theta) \otimes \text{purelin}(\mathbf{a})\right]\!\right]\right) \\ &= \text{IDFT}\left(\left[\!\left[\exp(j2\pi\Theta) \otimes \text{purelin}\left(\mathbf{w}_{\text{opt}}^T \boldsymbol{\phi}\right)\right]\!\right]\right), \end{aligned} \tag{33}$$

where purelin$(\cdot)$ is the output function of RBF network [37], $[\mathbf{z}]$ denotes the conjugate symmetric spectrum constructed from $\mathbf{z}$ which is the representative spectrum of the equivalent lowpass form [31]. The $N \times 1$ dimensional vector Θ represents the user defined phase response, and the operator $\otimes$ denotes the vector multiplication between the corresponding two vectors.

As is well known, orthogonal waveforms allow multiple UWB sensors to access the same idle band at the same time and in the same location, without causing serious collision. In a UWB sensor network, therefore, the orthogonal waveform division multiple accessing (WDMA) can also greatly simplify the upper layer protocol design and reduce accessing delay, hence significantly reducing scheduling complexity and improving spectrum efficiency.

For convenience, we assume that the emission power in idle frequency band is only related with the hardware specification of UWB devices. When the idle spectrum is detected, the emitted waveform remains a constant power, denoted by A, in the unused spectrum. For arbitrary two

orthogonal waveforms $h_1(t)$ and $h_2(t)$ with their Fourier transform denoted by $H_1(f)$ and $H_2(f)$, respectively, we have $\int_f H_1(f)H_2^*(f)df$ [31]. So, the following relation should be satisfied:

$$A^2 \int_B \exp(-j2\pi\theta_i(f)) \exp\left(j2\pi\theta_j(f)\right) df = 0, \quad (34)$$

where B is the available frequency bands. It can be found that careful design of the phase response $\theta_i(f)$ can produce the mutual orthogonal UWB waveforms. One simple scheme is to let the phase response to be

$$\theta_i(f) = \frac{1}{4} c_i(f). \quad (35)$$

Here, we specify $c_i(k)$ to be a binary sequence, for example, $c_i(k) \in \{-1, 1\}$. Then, the designed UWB waveforms will keep orthogonal with each other so long as to ensure orthogonality of discrete sequence $c_i(k)$. If an appropriate pseudorandom sequence, such as *m-sequence*, is selected based on the length of sampling length N, orthogonal UWB waveforms can be easily derived.

It is noted that from (34) the orthogonality design requires UWB signal remain constant in the whole frequency axis. If the regulatory UWB emission mask is taken into account, such as the FCC emission limits, however, this algorithm has to be further modified. Practically, we may represent the whole spectral line by a combination of constant spectral lines along the frequency axis. Thus, this orthogonality design algorithm is still applicable to each constant spectrum.

3. Numerical Simulations and Evaluations

In this part, we evaluate the performance of our presented algorithms through numerical simulations, both for the spectrum sensing and the UWB waveform sculpting.

3.1. Numerical Results for Spectrum Sensing. In our analysis, the number of sampling points M is set to 80. With respect to the service traffic parameters (μ, λ), corresponding to busy state and idle state of PU, we select five sets of parameters combination to comprehensively study the influence from model parameters on detection performance, which are as follows: (1) $\mu = 1, \lambda = 1$; (2) $\mu = 1/8, \lambda = 1/2$; (3) $\mu = 1/8, \lambda = 1/3$; (4) $\mu = 1/8, \lambda = 1/5$; (5) $\mu = 1/8, \lambda = 1/8$. Another group parameters combination is also used for systematical analysis.

3.1.1. Sensing Performance. According to the optimal decision threshold, the spectrum detection performance is obtained as is shown in Figure 3(a). When the traffic parameters are set to $\mu = \lambda = 1$, as we expected, the performance of our sequence detection based sensing algorithm is the same as ED. That is because *prior* information carried by state transition can be basically ignored in this case, and the state symbols in adjacent two sensing periods are approximately independent. So, the MAP criterion degenerates to ML detection, as is done by ED. When either μ or λ is larger than 1, however, it is obvious that the presented algorithm outperforms ED. Specifically, when the service parameters are $(\mu = 1/8, \lambda = 1/3)$, our proposed algorithm is about 2.2 dB better than ED, and 1.2 dB when $(\mu = 1/8, \lambda = 1/5)$. Another five parameters sets are also selected for penetrated discussions, as is depicted in Figure 3(b).

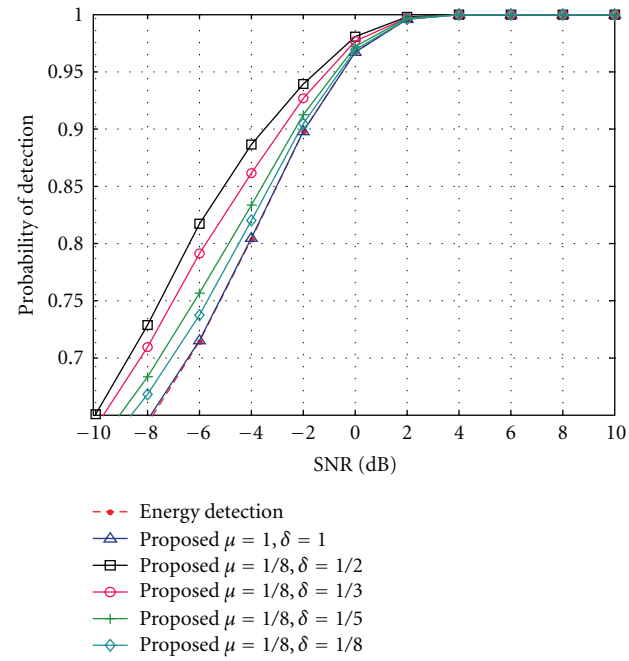

(a)

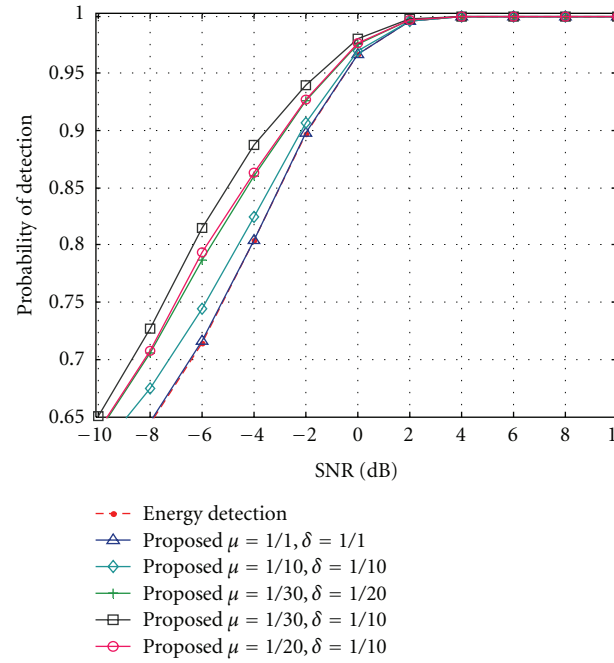

(b)

Figure 3: The detection performance of the proposed algorithm.

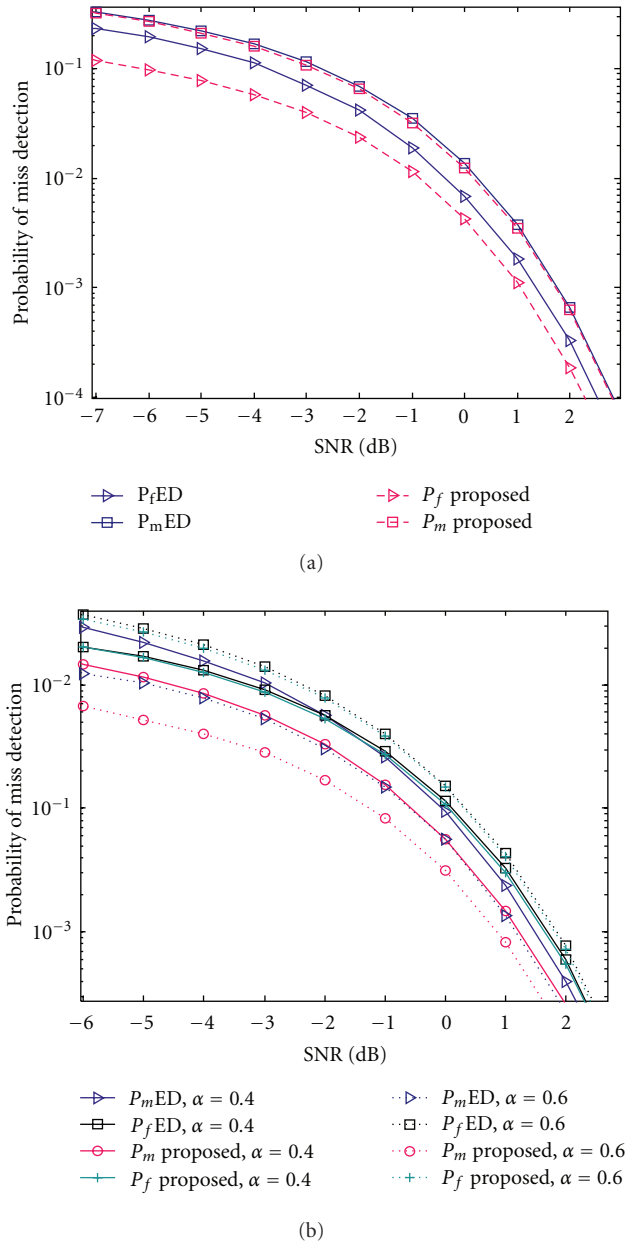

FIGURE 4: The missed detection and false alarm probabilities under different preferences.

Actually, as we discussed before, the performance improvement is mainly attributed to the potential *coding gain* caused by the hidden state transition of PU. Theoretically, the achievable gain is related to the *minimum code distance* of its corresponding finite state machine [29]. Consider that the state transition here is inhomogeneous, which means that the state transition probabilities change over time, and we can hardly employ a transition matrix to describe it, which also brings in great difficulty in analyzing the minimum code distance. Alternatively, we seek to reveal the interrelationship between the detection gain and the service traffic parameters from a quantitative angle by numerical simulations. From simulations in Figure 3(a), we note the following. (1) When the state parameters are ($\mu = 1/8$, $\lambda = 1/2$) and ($\mu = 1/8$, $\lambda = 1/5$), the detection performance can be increased by 2.2 dB and 1.2 dB, respectively. The same results are observed in Figure 3(b). Therefore, it can be concluded that the performance improvement in spectrum sensing is related to the ratio between states duration periods λ/μ. The larger this duration ratio is, the better the sensing gain is. In an extreme case that the ration tends to be infinite, which means that only one state exists, totally correct detection can be achieved going with the common sense. (2) In comparison with ED, when the state parameters are ($\mu = 1/8$, $\lambda = 1/8$) and ($\mu = 1/10$, $\lambda = 1/10$), the detection performance can be increased by 0.7 dB and 0.95 dB, respectively. So, we may say that the detection performance is improved with the increase of cycle duration. However, what to be emphasized is that the sensing gain caused by the increase of state duration is much less than that of by improving the ratio λ/μ. The reason is that the increase of state duration is equivalent to *repeat coding*; however, the improvement of λ/μ implies the minimum coding distance being aggregated. Hence, the achieved coding gain in the former case is limited relatively. Observation from Figure 3 shows that given the service parameters, slight enhancement in spectrum sensing can be obtained by only increasing the observed states duration, which is realized by shortening sensing-transmission period or increasing sampling rates.

3.1.2. Different Preferences. For different preferences between false alarm probability and missed probability, the relation between the sensing performance and signal noise ratio (SNR) is depicted in Figure 4. When α is chosen to 0.5, it is apparent that the false alarm probability has been significantly reduced while the missed probability remains unchanged. Compared to Neyman-Pearson criterion, our algorithm can increase the utilization efficiency of unused spectrum substantially while basically keeps the interference to licensed band the same as ED. Accordingly, the capacity of UWB sensor networks can be improved, which is rather beneficial to the urgent data transmission. On the other hand, if we put emphasis on missed probability and let α be 0.4, the false probability of this new algorithm is the same as ED; but the detection probability has been obviously enhanced. So, we can provide a much more reliable communication link to other legal networks. If we relatively prefer the missed probability and set α to 0.6, as is shown in Figure 4(b), although the detection probability of this algorithm remains close to ED, the false alarm is significantly optimized, which is resemble that of $\alpha = 0.5$.

3.1.3. Performance with Detection Errors. Figure 5 gives the sensing performance when the state estimation errors exist. In this simulation, we assume that the detection probability P is .8 and the traffic parameters are set as $\mu = 1/30$, $\lambda = 1/20$. It is shown that, when the state transition point error estimation gets earlier, the sensing performance will be declined by 0.61 dB compared to the ideal situation that the state transition moment has been precisely identified. On the other hand, if the state transition errors happen

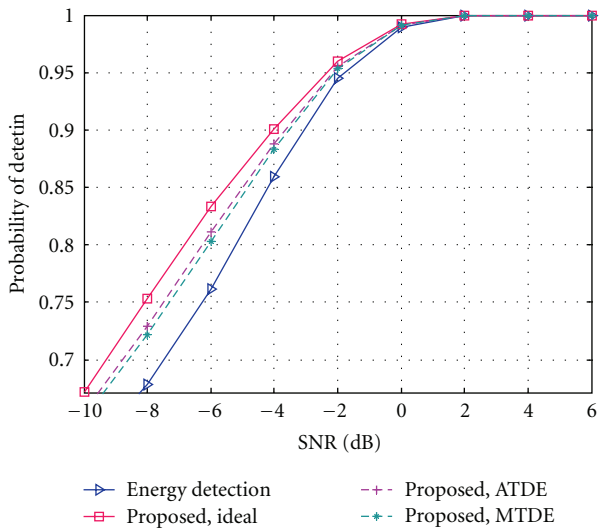

Figure 5: Detection performance with state transition estimation errors.

far away from the actual transition moment, the detection performance would decline by 0.75 dB. As a whole, however, the transition point detection error has little effect on sensing performance when the mean detection probability is high; so our proposed algorithm is robust to state estimation errors to some extent.

3.2. Numerical Results for Spectrum Sculpting. In UWB waveform generation simulations, the length of the basis function N is 180, the equivalent filter order n_2 is 32, and the shift factor l is 8. We note from the simulations that the UWB pulse can probably reach its convergence after 50 iterations. The out-band attenuation can be further optimized after total 100 iterations. Therefore, our proposed network has a fast convergence. Consequently, the switching time can be considerably shortened. Hence, with little accessing delay, the utilization of idle spectrum can be enhanced.

3.2.1. UWB Waveforms without Emission Limits. The power spectrum density (PSD) of the designed UWB signal is illustrated in Figure 6. Also, notice that the maximum frequency has been normalized. We assume that there is no spectral emission limit on UWB sensors, and the available spectrum locates at [0.17 0.33] and [0.52 0.82]. This situation mainly corresponds to certain applications where only some geographical adjacent networks operate nearby UWB sensors simultaneously. When adopting the simplified algorithm, with both κ_i *and* δ optimized beforehand, the obtained spectrum efficiency of UWB waveforms is about 95%. The spectral attenuation in corresponding primary bands is about 66 dB, which can essentially mitigate out-band interference to other networks. By contrast, the frequency hopping technique can only use one single frequency band, and the maximum spectrum efficiency is no more than 60% in this situation.

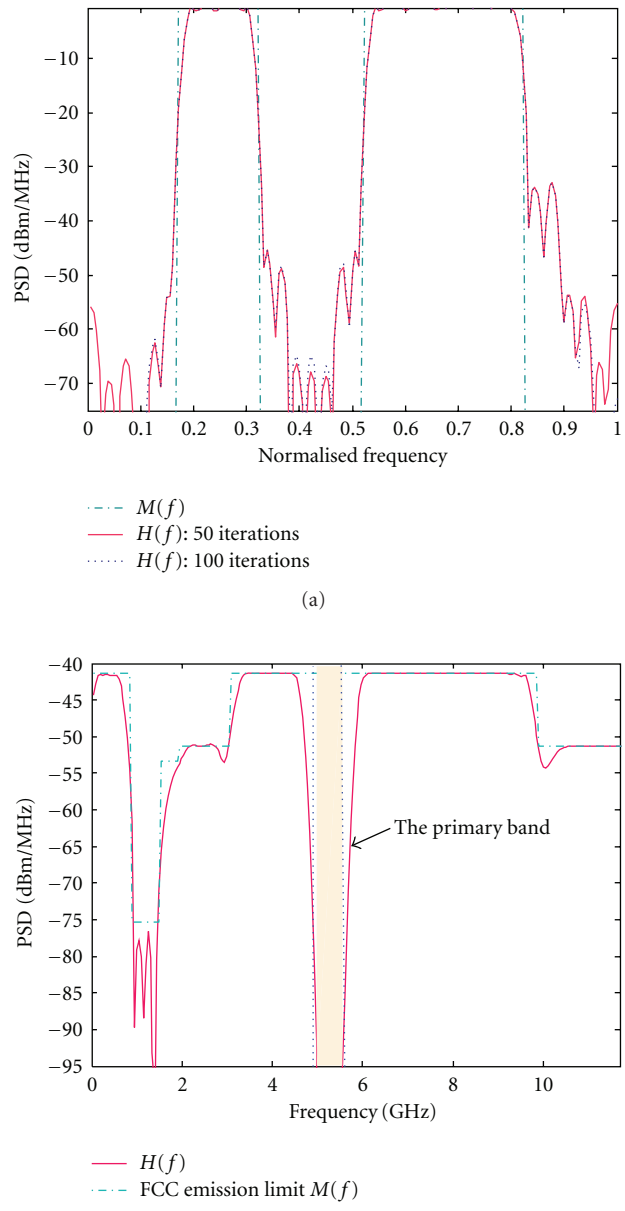

Figure 6: The designed UWB signals under different applications. (a) UWB waveform without regulatory emission limits. (b) UWB waveforms under FCC emission template. Notice that the total number of the basis functions is 64 in (b).

3.2.2. UWB Waveforms with Emission Limits. On the other hand, the UWB signal in Figure 6(b) is emitted under a strictly regulatory emission mask in order to avoid interfering other legal wireless services in indoor applications. Here, we adopt the FCC emission mask [11]. At the same time, recent investigations indicated that there may still exist unbearable interference to some specific legal services even if the emitted pulse has adopted the regulatory emission limit [13]. Therefore, the transmit UWB pulses should perform sufficient spectrum avoidance to further eliminate its potential interference to these specific wireless systems.

It can be found that, even in this situation, UWB signal can still take full advantage of the regulatory spectrum to improve its communication reliability. As is shown by Figure 6(b), spectrum efficiency can be as much as 97.6% in unoccupied bands. We also assume that there is one active legal network being detected in [5 5.5] GHz. With little effort, the corresponding subweight vector, denoted by $\mathbf{w}_{\text{avoid}}$, can be determined from (31) with f_{down} and f_{up} replaced by the vulnerable band. Then by directly setting $\mathbf{w}_{\text{avoid}}$ to 0, the UWB waveform with spectrum notch can be generated as shown in Figure 6(b). Spectral notches with attenuation larger than 90 dB can be produced, which effectively eliminates the interference from UWB sensors to other networks. Besides, other networks' signals are usually equivalent to narrow-band interference for UWB sensors; so this spectrum notch can be also employed to mitigate the narrow-band interference. In comparison, the obtained spectrum efficiency of the Hermite-Gaussian function based UWB waveform is only 65%, and the spectral attenuation in primary band is 25 dB [22]. The designed shaping filter in [23] can generate UWB waveforms with a spectrum efficiency of 83.7%. However, given a specific primary user over its working band, the spectral attenuation may be only 30 dB at the expense of the obvious spectrum efficiency decline in nonprimary bands. When the aggregate emission energy from multiple UWB nodes is considered, these exited schemes can hardly mitigate mutual interference between UWB sensors and other legal networks.

3.2.3. Orthogonal UWB Waveforms. Furthermore, orthogonal UWB waveforms can be easily designed based on our suggested method. Taking FCC emission limits for example, we firstly divide the whole emission mask into multiple nonoverlapped spectral sections with constant amplitude. Then, by carefully designing the corresponding phase response for each spectral line, the orthogonal pulses can be derived. The correlation as well as autorelation of orthogonal UWB waveforms is illustrated in Figure 7(a). Multiple UWB sensors apparently keep mutual orthogonal when the accurate synchronization has been acquired. Once spectrum holes are detected, UWB sensors can access without waiting for a coordinate control. So, our orthogonal waveforms can be applied to UWB sensors to significantly reduce complexity of the upper layer control so as to avoid unacceptable scheduling delay. Moreover, it should be noted that the correlation in essence remains zero within a certain synchronization derivation range (about 0.4 nanoseconds). As a result, in multiple UWB sensor networks with the timing errors, the performance of our UWB waveforms is supposed to be much superior to that of based on SOCP [23].

In Figure 7(b), we evaluate the transmission performance of existing different waveforms in a UWB network which is based on WDMA. In this experiment, we still adopt FCC emission mask and the maximum UWB frequency is 12 GHz. The uncoded binary pulse amplitude modulation (PAM) is adopted in the transmitter, and the coherent correlator

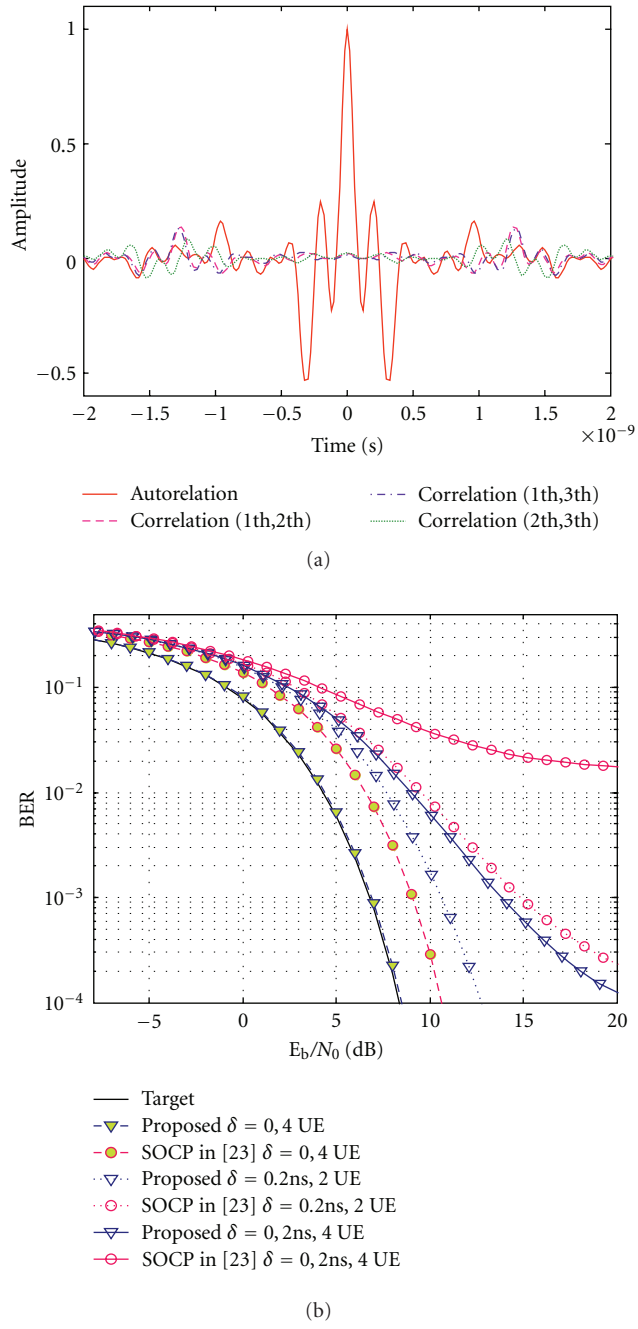

FIGURE 7: (a) Orthogonality illustrations of the designed waveforms. (b) Transmission performance of different UWB signals in a WDMA network. Note that target performance corresponds to the ideal UWB pulse, with spectral efficiency of 1.

is employed to perform optimal receiving in the presence of AWGN. It is demonstrated from this simulation that the BER performance of our proposed pulses, operating in 4-user WDMA network, can surpass SOCP technique about 2 dB [23], if accurate timing has been acquired in UWB receivers. When there is timing inaccuracy in UWB receivers, the designed pulses can obtain about 9 dB gain compared to SOCP-based orthogonal pulses, when the

maximum timing deviation is about 0.2 nanoseconds in 2-user WDMA network and the BER drops below 10^{-4}. Therefore, from the aspect of the whole UWB network performance, our scheme can indeed enhance transmission performance and reduce stringent requirement on networks synchronization, thus simplifying UWB receiver complexity. Notice that, here, we only show the performance in AWGN channel. As is discussed in [38], on the other hand, noncoherent receiver is much more suitable for a simple UWB implementation, and in this case, BER performance is closed related to spectral energy carried by single UWB waveforms. Hence, our UWB signal is still supposed to outperform other methods given the UWB emission limits.

4. Conclusion

We address the coexistence issues between UWB sensors and others networks in this paper. A cognitive-based dynamic spectrum accessing scheme is suggested to mitigate mutual interference between geographic adjacent networks, in which UWB sensors utilize available idle spectrums by monitoring the nearby spectral environment and identifying the unused spectrum. By introducing state transition process to describe the working state of PU, we transform spectrum sensing into the demodulation of an equivalent state sequence. In fact, our presented algorithm provides a new insight in general spectrum sensing which may benefit other specific sensing algorithms. To react to the highly emission adaptation in UWB sensors, a signal generator with great reconfigurable capability is proposed based on RBF network. The designed UWB waveforms can entirely utilize multiple spectral sections to improve the transmission reliability of UWB sensors. Also, our algorithm can produce signals with sufficient spectrum avoidance and totally eliminate mutual interference between nearby networks and UWB sensors. The orthogonal cognitive UWB waveform is also investigated finally. It can be found that, in WDMA-based UWB sensor networks with timing deviation, our orthogonal waveforms considerably outperform other existed UWB orthogonal signals. Future work may include profound analysis on sensing performance in the presence of state estimation errors. Also, the accurate relation between sensing gain and the PU state transition characteristic remains an attractive area in following investigations.

Acknowledgments

This research was partly supported by the Ministry of Knowledge Economy, South Korea, under the ITRC support program supervised by the Institute for Information Technology Advancement (IITA-2009-C1090-0902-0019). This work was supported by NSFC (60772021, 60972079, 60902046), the Research Fund for the Doctoral Program of Higher Education (20060013008, 20070013029), and the National High-tech Research and Development Program (863 Program) (2009AA01Z262).

References

[1] P. Withington, H. Fluhler, and S. Nag, "Enhancing homeland security with advanced UWB sensors," *IEEE Microwave Magazine*, vol. 4, no. 3, pp. 51–58, 2003.

[2] S. Nag, M. A. Barnes, T. Payment, and G. W. Holladay, "An ultra-wideband through-wall radar for detecting the motion of people in real time," in *Radar Sensor Technology and Data Visualisation*, vol. 4744 of *Proceedings of SPIE*, pp. 48–57, Orlando, Fla, USA, 2002.

[3] "Ground Penetrating Radar," http://www.geo-sense.com/GPR.htm.

[4] J. Liang, Q. Liang, and S. W. Samn, "Foliage clutter modeling using the UWB radar," in *Proceedings of the IEEE International Conference on Communications*, pp. 1937–1941, Beijing, China, 2008.

[5] J. Liang, Q. Liang, and S. W. Samn, "A propagation environment modeling in foliage," *EURASIP Journal on Wireless Communications and Networking*, vol. 2010, Article ID 873070, 12 pages, 2010.

[6] Q. Liang, S. W. Samn, and X. Cheng, "UWB radar sensor networks for sense-through-foliage target detection," in *Proceedings of the IEEE International Conference on Communications*, pp. 2228–2232, Beijing, China, May 2008.

[7] J. Liang, Q. Liang, S. W. Samn, and R. Narayanan, "A differential based approach for sense-through-foliage target detection using UWB radar sensor networks," in *Proceedings of the IEEE International Conference on Communications*, pp. 1952–1956, Beijing, China, May 2008.

[8] J. Liang and Q. Liang, "UWB radar sensor networks detection of targets in foliage using short-time Fourier transform," in *Proceedings of the IEEE International Conference on Communications*, pp. 1–5, Dresden, Germany, June 2009.

[9] J. Liang, Q. Liang, and S. W. Samn, "Sense-through-wall channel modeling using UWB noise radar," in *Proceedings of IEEE International Workshop on Multi-Gigabit MM-Wave and Tera-Hz Wireless Systems (GlOBECOM '09)*, Honolulu, Hawaii, USA, November 2009.

[10] P. Cheolhee and T. S. Rappaport, "Short-range wireless communications for next-generation networks: UWB 60 GHz millimeter-wave wpan, and ZigBee," *IEEE Wireless Communications*, vol. 14, no. 4, pp. 70–78, 2007.

[11] Q. Ren and Q. Liang, "Throughput and energy-efficiency aware ultra wideband communication in wireless sensor networks: a cross-layer approach," *IEEE Transactions on Mobile Computing*, vol. 7, no. 7, pp. 805–816, 2008.

[12] Federal Communications Commission (FCC), "Revision of part 15 of the commission's rules regarding ultra-wide band transmission systems," First Report and Order ET Docket 98-153, FCC 02–48, 2002.

[13] R. Giuliano and F. Mazzenga, "On the coexistence of power-controlled ultrawide-band systems with UMTS, GPS, DCS1800, and fixed wireless systems," *IEEE Transactions on Vehicular Technology*, vol. 54, no. 1, pp. 62–81, 2005.

[14] S. Haykin, "Cognitive radio: brain-empowered wireless communications," *IEEE Journal on Selected Areas in Communications*, vol. 23, no. 2, pp. 201–220, 2005.

[15] F. F. Digham, M.-S. Alouini, and M. K. Simon, "On the energy detection of unknown signals over fading channels," in *Proceedings of the IEEE International Conference on Communications*, vol. 5, pp. 3575–3579, Anchorage, Alaska, USA, May 2003.

[16] D. Cabric, S. M. Mishra, and R. W. Brodersen, "Implementation issues in spectrum sensing for cognitive radios," in *Proceedings of the Asilomar Conference on Signals, Systems and Computers*, vol. 1, pp. 772–776, Pacific Grove, Calif, USA, November 2004.

[17] W. A. Gardner, "Exploitation of spectral redundancy in cyclostationary signals," *IEEE Signal Processing Magazine*, vol. 8, no. 2, pp. 14–36, 1991.

[18] R. Tandra and A. Sahai, "Fundamental limits on detection in low SNR under noise uncertainty," in *Proceedings of the 25th International Conference on Wireless Networks, Communications and Mobile Computing*, vol. 1, pp. 464–469, June 2005.

[19] Z. Tian and G. B. Giannakis, "A wavelet approach to wideband spectrum sensing for cognitive radios," in *Proceedings of the 1st International Conference on Cognitive Radio Oriented Wireless Networks and Communications (CROWNCOM '06)*, pp. 1–5, Island, Greece, June 2006.

[20] Y. Zeng and Y.-C. Liang, "Spectrum-sensing algorithms for cognitive radio based on statistical covariances," *IEEE Transactions on Vehicular Technology*, vol. 58, no. 4, pp. 1804–1815, 2009.

[21] H. Zhang, X. Zhou, K. Y. Yazdandoost, and I. Chlamtac, "Multiple signal waveforms adaptation in cognitive ultra-wideband radio evolution," *IEEE Journal on Selected Areas in Communications*, vol. 24, no. 4, pp. 878–884, 2006.

[22] R. Yang, Z. Zhou, L. Zhang, and C. Yu, "Detection and avoidance scheme for direct-sequence ultra-wideband system: a step towards cognitive radio," *IET Communications*, vol. 2, no. 8, pp. 1043–1050, 2008.

[23] X. Wu, Z. Tian, T. N. Davidson, and G. B. Giannakis, "Optimal waveform design for UWB radios," *IEEE Transactions on Signal Processing*, vol. 54, no. 6, pp. 2009–2021, 2006.

[24] I. Dotlic and R. Kohno, "Design of the family of orthogonal and spectrally efficient UWB waveforms," *IEEE Journal on Selected Topics in Signal Processing*, vol. 1, no. 1, pp. 21–30, 2007.

[25] V. D. Chakravarthy, A. K. Shaw, M. A. Temple, and J. P. Stephens, "Cognitive radio—an adaptive waveform with spectral sharing capability," in *Proceedings of the IEEE Wireless Communications and Networking Conference (WCNC '05)*, vol. 2, pp. 724–729, New Orleans, La, USA, March 2005.

[26] J. Ma, G. Y. Li, and B. H. Juang, "Signal processing in cognitive radio," *Proceedings of the IEEE*, vol. 97, no. 5, pp. 805–823, 2009.

[27] J. Ma and Y. Li, "A probability-based spectrum sensing scheme for cognitive radio," in *Proceedings of the IEEE International Conference on Communications*, Proceedings of SPIE, pp. 3416–3420, Beijing, China, May 2008.

[28] X. Zhou, J. Ma, G. Y. Li, Y. H. Kwon, and A. C. K. Soong, "Probability-based optimization of inter-sensing duration and power control in cognitive radio," *IEEE Transactions on Wireless Communications*, vol. 8, no. 10, pp. 4922–4927, 2009.

[29] W. Zhang and K. Letaief, "Cooperative spectrum sensing with transmit and relay diversity in cognitive radio networks," *IEEE Transactions on Wireless Communications*, vol. 7, no. 12, pp. 4761–4766, 2008.

[30] K. B. Letaief and W. Zhang, "Cooperative communications for cognitive radio networks," *Proceedings of the IEEE*, vol. 97, no. 5, pp. 878–893, 2009.

[31] J. G. Proakis, *Digital Communications*, McGraw-Hill, New York, NY, USA, 4th edition, 2001.

[32] B. Vujitic, N. Cackov, and S. Vujitic, "Modeling and characterization of traffic in public safety wireless network," in *Proceedings of the International Symposium on Performance Evaluation of Computer and Telecommunication Systems*, pp. 213–223, Edinburgh, UK, July 2005.

[33] A. Papoulis, *Probability, Random Variables, and Stochastic Process*, McGraw-Hill, New York, NY, USA, 4th edition, 2002.

[34] S. Geirhofer, L. Tong, and B. M. Sadler, "Cognitive medium access: constraining interference based on experimental models," *IEEE Journal on Selected Areas in Communications*, vol. 26, no. 1, pp. 95–105, 2008.

[35] B. Li, Z. Zhou, and W. Zou, "A novel spectrum adaptive UWB pulse: application in cognitive radio," in *Proceedings of IEEE Vehicular Technology Conference (VTC '09)*, pp. 1–5, Anchorage, Alaska, USA, September 2009.

[36] B. Li, W. Zou, and Z. Zhou, "A novel adaptive spectrum forming filter: application in cognitive ultra wideband radio," *Science China Information Science*. Accepted for publication.

[37] S. Haykin, *Neural Networks: A Comprehensive Foundation*, Prentice-Hall, Upper Saddle River, NJ, USA, 2nd edition, 1998.

[38] K. Witrisal, G. Leus, G. J. M. Janssen, et al., "Noncoherent ultra-wideband systems," *IEEE Signal Processing Magazine*, vol. 26, no. 4, pp. 48–66, 2009.